J Physiol 590.23 (2012) pp 5993–6011

The Journal of Physiology

PIP_2 hydrolysis stimulates the electrogenic Na^+–bicarbonate cotransporter NBCe1-B and -C variants expressed in *Xenopus laevis* oocytes

Ian M. Thornell[1], Jianping Wu[1], Xiaofen Liu[1] and Mark O. Bevensee[1,2,3,4]

[1]*Department of Cell, Developmental and Integrative Biology,* [2]*Nephrology Research and Training Center,* [3]*Center of Glial Biology in Medicine, and* [4]*Civitan International Research Center, University of Alabama at Birmingham, Birmingham, AL 35294, USA*

Key points

- The Na^+–bicarbonate cotransporter NBCe1 regulates cell and tissue pH, as well as ion movement across cell layers in organs such as kidney, gut, and pancreas.
- We previously showed that the signalling molecule PIP_2 stimulates the cloned A variant of NBCe1 in a patch of biological membrane.
- In the current study, we characterize the effect of injecting PIP_2 into intact oocytes expressing an NBCe1 variant (A, B, or C).
- PIP_2 stimulates the B and C variants, but not the A variant, through hydrolysis to IP_3. Stimulation requires an intracellular Ca^{2+} store and kinase activity.
- The results will contribute to our understanding of multiple HCO_3^--dependent transporters with different modes of regulation, as well as how molecules that stimulate specific membrane receptors lead to changes in cell/tissue pH, and perhaps how pathologies such as stroke and ischaemia that lead to energy deficiency cause tissue acidosis.

Abstract Electrogenic Na^+–bicarbonate cotransporter NBCe1 variants contribute to pH_i regulation, and promote ion reabsorption or secretion by many epithelia. Most Na^+-coupled bicarbonate transporter (NCBT) families such as NBCe1 contain variants with differences primarily at the cytosolic N and/or C termini that are likely to impart on the transporters different modes of regulation. For example, N-terminal regions of NBCe1 autoregulate activity. Our group previously reported that cytosolic phosphatidylinositol 4,5-bisphosphate (PIP_2) stimulates heterologously expressed rat NBCe1-A in inside-out macropatches excised from *Xenopus laevis* oocytes. In the current study on whole oocytes, we used the two-electrode voltage-clamp technique, as well as pH- and voltage-sensitive microelectrodes, to characterize the effect of injecting PIP_2 on the activity of heterologously expressed NBCe1-A, -B, or -C. Injecting PIP_2 (10 μM estimated final) into voltage-clamped oocytes stimulated NBC-mediated, HCO_3^--induced outward currents by >100% for the B and C variants, but not for the A variant. The majority of this stimulation involved PIP_2 hydrolysis and endoplasmic reticulum (ER) Ca^{2+} release. Stimulation by PIP_2 injection was mimicked by injecting IP_3, but inhibited by either applying the phospholipase C (PLC) inhibitor U73112 or depleting ER Ca^{2+} with prolonged thapsigargin/EGTA treatment. Stimulating the activity of store-operated Ca^{2+} channels (SOCCs) to trigger a Ca^{2+} influx mimicked the PIP_2/IP_3 stimulation of the B and C variants. Activating the endogenous G_q protein-coupled receptor in oocytes with lysophosphatidic acid (LPA) also stimulated the B and C variants in a Ca^{2+}-dependent manner, although via an increase in surface expression for the B variant. In simultaneous voltage-clamp and pH_i studies

DOI: 10.1113/jphysiol.2012.242479

on NBCe1-C-expressing oocytes, LPA increased the NBC-mediated pH_i-recovery rate from a CO_2-induced acid load by ∼80%. Finally, the general kinase inhibitor staurosporine completely inhibited the IP_3-induced stimulation of NBCe1-C. In summary, injecting PIP_2 stimulates the activity of NBCe1-B and -C expressed in oocytes through an increase in IP_3/Ca^{2+} that involves a staurosporine-sensitive kinase. In conjunction with our previous macropatch findings, PIP_2 regulates NBCe1 through a dual pathway involving both a direct stimulatory effect of PIP_2 on at least NBCe1-A, as well as an indirect stimulatory effect of IP_3/Ca^{2+} on the B and C variants.

(Received 3 August 2012; accepted after revision 4 September 2012; first published online 10 September 2012)
Corresponding author M. O. Bevensee: Department of Cell, Developmental and Integrative Biology, University of Alabama at Birmingham, 1918 University Blvd, 812 MCLM, Birmingham, AL 35294-0005, USA. Email: bevensee@uab.edu

Abbreviations AE, anion exchanger; BTR, bicarbonate transporter-related protein; DAG, diacylglycerol; GPCR, G-protein coupled receptor; HA, haemagglutinin; IRBIT, IP_3 receptor binding protein released with IP_3; LPA, lysophosphatidic acid; NBCe, electrogenic Na^+–bicarbonate cotransporter; NBCn, electroneutral Na^+–bicarbonate cotransporter; NCBT, Na^+-coupled bicarbonate transporter; NCBE, Na^+-driven Cl^-–bicarbonate exchanger; NDCBE, Na^+-driven Cl^-–bicarbonate exchanger; PIP_2, phosphatidylinositol 4,5-bisphosphate; PLC, phospholipase C; PKA, phosphokinase A; PKC, phosphokinase C; Pretx, pretreatment; SOC, single-oocyte chemiluminescence; SOCC, store-operated calcium channel; TG, thapsigargin.

Introduction

Na^+-coupled bicarbonate transporters (NCBTs) are powerful regulators of pH_i, and also contribute to trans-epithelial Na^+ and HCO_3^- reabsorption and secretion in epithelia. NCBTs include the following paralogues in the *Slc4* gene family (Romero *et al.* 2004): the electrogenic Na^+/HCO_3^- cotransporters NBCe1 (*Slc4a4*) and NBCe2 (*Slc4a5*), the electroneutral Na^+/HCO_3^- cotransporters NBCn1 (*Slc4a7*) and NBCn2/NCBE (*Slc4a10*), and the electroneutral Na^+-driven Cl^-–HCO_3^- exchanger NDCBE (*Slc4a8*). Additional paralogues in the gene family include the anion exchangers AE1–4 (*Slc4a1–3* and *-9*), and the less characterized borate transporter BTR1 (*Slc4a11*).

The diversity of the *Slc4* gene family is further enriched by different variants of the aforementioned paralogues. Differences of each NCBT paralogue are found at the cytoplasmic N- and/or C-termini. The one exception is NBCe2 with splice differences between predicted transmembrane domains 11 and 12. Regarding NBCe1, the A variant (NBCe1-A) contains 41 unique amino acids at the N terminus that arise from an alternative promoter in intron 3 of *Slc4a4* (Abuladze *et al.* 2000). NBCe1-B is identical to NBCe1-A except for 85 N-terminal residues that replace the 41 N-terminal residues of the A variant (Fig. 1). In a similar fashion, NBCe1-C is identical to NBCe1-B except for 61 unique C-terminal residues (due to a 97 base-pair deletion near the 3′ open reading frame) that replace the 46 C-terminal residues of the B variant (Bevensee *et al.* 2000). Recently, Liu *et al.* (2011) identified two additional NBCe1 splice variants that lack a nine-residue cassette in the cytoplasmic N terminus of either the A variant (NBCe1-D) or the B variant (NBCe1-E). In the current study, we focus on the A, B, and C variants with larger amino acid differences at the N and/or C termini.

Although the physiological significance of multiple NBCe1 variants has yet to be fully elucidated, the modular splicing may impart the transporter with different modes of regulation under various conditions or stimuli. Indeed, N-terminal regions of NBCe1 regulate transporter activity themselves and through associations with other molecules. For example, the unique N terminus of NBCe1-A contains an autostimulatory domain because its removal reduces transporter activity by ∼50% (McAlear *et al.* 2006). In contrast, the different N terminus of the B and C variants contains an autoinhibitory domain because its removal stimulates transporter activity by ∼3-fold. Regarding interacting proteins, Shirakabe *et al.* (2006) found that the IP_3 receptor binding protein released with inositol trisphosphate (IRBIT) binds to the N terminus and stimulates NBCe1-B, but not NBCe1-A. More recently, we found that IRBIT also stimulates the activity of NBCe1-C when co-expressed in *Xenopus* oocytes (Thornell *et al.* 2010). NBCe1 variants can be modulated by traditional signalling molecules such as protein kinase A (PKA)/cAMP (Gross *et al.* 2001; Gross *et al.* 2003), protein kinase C (PKC) (Perry *et al.* 2006), Ca^{2+} (Müller-Berger *et al.* 2001), and ATP (Heyer *et al.* 1999). One cAMP effect is variant specific as shown by Gross *et al.* (2003), who reported that a Thr at position 49 in the N terminus of human NBCe1-B (but not NBCe1-A) is required for a cAMP-stimulated increase in transporter activity. This increase, however, does not appear to involve a change in the Thr's phosphorylation state.

We hypothesize that other regulatory pathways may differentially affect the activity of the NBCe1 variants. We recently discovered that the membrane phospholipid PIP_2 reduces the rate of run-down and stimulates activity of heterologously expressed rat NBCe1-A in excised macropatches from *Xenopus* oocytes (Wu *et al.* 2009*b*). In the current study, we used the two-electrode voltage-clamp technique and pH/voltage-sensitive microelectrodes to characterize the effect of PIP_2 and its hydrolysis on the activity of all three rat NBCe1 variants heterologously expressed in intact oocytes. We find that injecting PIP_2 into oocytes stimulates the B and C variants —but not the A variant— through hydrolysis to IP_3. Stimulation by PIP_2 injection was eliminated by the PLC inhibitor U73122, and mimicked by either injecting IP_3 or activating the endogenous G_q-coupled receptor with lysophosphatidic acid (LPA). PIP_2/IP_3 stimulation was mediated by an increase in $[Ca^{2+}]_i$ because the stimulation was eliminated by depleting ER Ca^{2+} stores, and mimicked by activating store-operated Ca^{2+} channels (SOCCs). The IP_3 stimulation involves a staurosporine-sensitive kinase.

Portions of this work have been published in preliminary form (Wu *et al.* 2009*a*; Thornell *et al.* 2010; Thornell & Bevensee, 2011).

Methods

Ethical approval

The Institutional Animal Care and Use Committee (IACUC) at UAB reviewed and approved the protocol for harvesting oocytes from *Xenopus laevis* frogs.

Constructs and cRNA

cDNAs encoding NBCe1-A, -B, and -C, as well as $C_{\Delta N87}$, were previously subcloned into the oocyte expression vector pTLNII (McAlear *et al.* 2006). $C_{\Delta N87}$ is an NBCe1-C construct with its N-terminal 87 residues deleted (McAlear *et al.* 2006). All NBC constructs contained a nine-residue haemagglutinin (HA) epitope (YPYDVPDYA) in the exofacial loop between the fifth and sixth putative transmembrane domains that allowed us to analyse surface expression using single-oocyte chemiluminescence (SOC) as described below. IRBIT constructs obtained from others were also HA tagged.

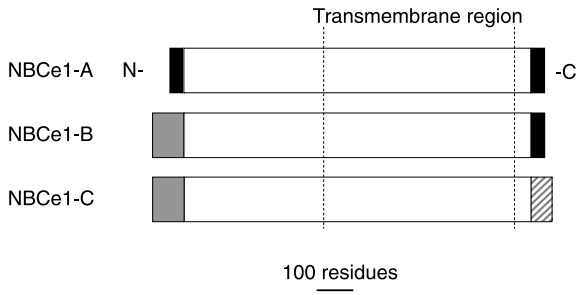

Figure 1. NBCe1-A, -B, and -C variants are identical except at the amino and/or carboxy termini
Eighty-five N-terminal residues of the B and C variants (grey) replace the unique 41 N-terminal residues of the A variant (black), and 61 C-terminal residues of the C variant (striped) replace the 46 C-terminal residues of the A and B variants (black). The transmembrane region denoted by the dotted lines contains as many as 14 transmembrane domains (Boron *et al.* 2009; Zhu *et al.* 2010).

pTLNII plasmids were linearized with *Mlu*I, purified with the DNA Clean & Concentrator-5 Kit (Zymo Research, Irvine, CA, USA), and then transcribed using the SP6 transcription kit (Ambion, Life Technologies, Grand Island, NY, USA). cRNA was purified using the RNeasy Mini kit (Qiagen, Valencia, CA, USA).

Oocytes

Oocytes were harvested from female *Xenopus laevis* frogs (Xenopus Express, Brooksville, FL, USA) as previously described (McAlear *et al.* 2006; McAlear & Bevensee, 2006). Segments of the ovarian lobe from anaesthetized female frogs (with 0.2% tricaine) were extracted through an incision in the abdominal cavity, teased apart into ~0.5 cm^2 pieces, and then digested for 1–1.5 h in sterile Ca^{2+}-free ND96 containing 2 mg ml^{-1} collagenase A (Roche Applied Science, Indianapolis, IN, USA). After the digested segments were washed in Ca^{2+}-free ND96 followed by Ca^{2+}-containing ND96, stage-V/VI oocytes were selected under a dissecting microscope (GZ6, Leica, Buffalo Grove, IL, USA). Frogs were monitored during their recovery period after surgery; frogs were humanely killed after a final oocyte collection. Some stage V/VI oocytes were supplied from Ecocyte Bioscience (Austin, TX, USA).

A Nanoject II microinjector (Drummond Scientific, Broomall, PA, USA) was used to inject individual oocytes with 48 nl of either RNase-free H_2O (null control) or cRNA-containing H_2O. Oocytes were incubated at 18°C in sterile ND96 supplemented with 10 mM sodium pyruvate and 10 mg ml^{-1} gentamycin.

Two-electrode voltage-clamp experiments

Our technique for using the two-electrode voltage-clamp technique to measure NBC currents has been previously described (McAlear *et al.* 2006; Liu *et al.* 2007). Briefly, voltage-sensitive and current-passing electrodes pulled from G83165T-4 borosilicate glass capillaries (Warner Instruments, Hamden, CT, USA) were filled with saturated KCl and attached to the appropriate channels of an OC-725C voltage-clamp apparatus (Warner Instruments). For real-time current recordings, oocytes were voltage clamped at −60 mV and signals

were filtered at 10–15 Hz with an eight-pole LFP-8 Bessel filter (Warner Instruments). The sampling frequency was 2 kHz; data were reduced by a factor of 100 using ClampFit (pCLAMP 8.2, Molecular Devices, San Jose, CA, USA). For current–voltage (*I–V*) data, oocytes were voltage clamped at −60 mV between voltage-step protocols, and unfiltered amplifier signals (10 kHz) were sampled at 2 kHz. The voltage-step protocol consisted of 13 sweeps with a starting voltage of −60 mV for 12.5 ms, then a step to one of 13 voltages (−180 mV to 60 mV in increments of 20 mV) for 75 ms, and finally a return to −60 mV for 35 ms before the next sweep. ClampEx software (pCLAMP 8.2, Molecular Devices) controlled the acquisition, and a 1322A interface digitized the data (Molecular Devices). ClampFit software was used to analyse the data.

Experiments were performed at room temperature on oocytes at least 2 days after cRNA injection. Oocytes were placed in a continuous flow chamber connected to a custom-designed, gravity-fed solution delivery system. Solutions delivered to the chamber (∼500 μl volume) were controlled by a pair of six-way rotary valves with outputs converging at a two-position, four-way Hamilton valve close to the chamber. This two-position valve allowed us to alternate which six-way rotary valve delivered solution to the perfusion chamber *vs.* waste (for priming purposes). The solution flow rate was 4–6 ml min^{-1}. In injection experiments, oocytes were also impaled at the vegetal-animal pole equator with a micropipettor attached to a Nanoject II microinjector to inject PIP_2, IP_3, or H_2O.

Simultaneous pH_i and voltage-clamp experiments

We measured pH_i using pH- and voltage-sensitive microelectrodes as previously described (McAlear *et al.* 2006), but with a modified approach to voltage-clamp simultaneously. To make pH-sensitive microelectrodes, G200F-4 borosilicate glass capillaries (Warner Instruments) were first acid-washed and baked at 200°C. Capillaries were then pulled with a Brown–Flaming micropipette puller (P-80, Sutter Instrument Co., Novato, CA, USA), and baked again before being silanized with *bis*-(methylamino)dimethylsilane (Fluka/Sigma-Aldrich, St Louis, MO, USA). Electrode tips were filled with hydrogen ionophore I-cocktail B (Fluka/Sigma-Aldrich), and the electrodes backfilled with a pH-7.0 solution containing 150 mM NaCl, 40 mM KH_2PO_4, and 23 mM NaOH. pH electrodes were then connected to one channel of an FD223 high-impedance electrometer (WPI, Sarasota, FL, USA). The pH signal was obtained with a four-channel electrometer (Biomedical Instrumentation Laboratory, Department of Cellular and Molecular Physiology, Yale University, New Haven, CT, USA) that subtracted the 10× voltage output from the oocyte clamp (after split and relay through a 10× voltage divider) from the potential of the pH electrode. In voltage-clamp mode, the virtual ground clamps the bath potential to 0 mV, so the voltage output (or V_m) equals the potential of the voltage electrode. Junction potentials were minimized with 3% agar/saturated KCl bridges (made of ∼1 cm cut glass capillaries) between the virtual ground wires and bath solution. Digitized pH and voltage signals were acquired and plotted using custom-designed software written by Mr Duncan Wong for the W. F. Boron laboratory (formerly in the Department of Cellular and Molecular Physiology, Yale University). Before each experiment, the pH electrode was calibrated in the recording chamber with pH-6 and -8 buffer solutions (Fisher Scientific, Pittsburgh, PA, USA).

Solutions

The standard ND96 solution (pH 7.5) contained (in mM): 96 NaCl, 2 KCl, 1 $MgCl_2$, 1.8 $CaCl_2$, 5 Hepes, and 2.5 NaOH. In the standard 5% CO_2–33 mM HCO_3^- solution, 33 mM NaCl was replaced with an equimolar amount of $NaHCO_3$, and the solution was equilibrated with 5% CO_2–95% O_2 to pH 7.5. In Ca^{2+}-free ND96 and 5% CO_2–33 mM HCO_3^- solutions, 1.8 mM $CaCl_2$ was replaced with 4 mM $MgCl_2$ + 1 mM EGTA. All chemicals and drugs were obtained from Sigma-Aldrich unless otherwise noted. All lipids were obtained from Avanti Polar Lipids (Pelham, AL, USA).

Single-oocyte chemiluminescence

Our technique for measuring surface expression of NBCe1 variants by SOC has been previously described (McAlear *et al.* 2006; McAlear & Bevensee, 2006). Oocytes were fixed with 4% paraformaldehyde and incubated overnight in a 1% BSA-ND96 blocking solution, and then incubated for 1 h in a blocking solution containing a 1:100 dilution of the rat monoclonal α-hemagglutinin (HA) antibody (Roche), and then one containing a 1:400 dilution of the secondary antibody, goat α-rat IgG-HRP (Jackson ImmunoResearch Laboratories, West Grove, PA, USA). The aforementioned incubations were performed with sterile solutions at 4°C. Individual oocytes were incubated in 50 μl SuperSignal Elisa Femto substrate (Pierce/Thermo Scientific, Rockford, IL, USA) for ∼1 min in an Eppendorf tube before luminescence was measured with a TD-20/20 luminometer (Turner Designs, Sunnyvale, CA, USA) for 15 s.

Immunoblotting of oocyte protein

Total protein was isolated by first homogenizing oocytes with a pestle in 20 μl per oocyte of a homogenization buffer (100 mM NaCl, 1% Triton X-100, 20 mM Tris-HCl,

and 10 mM methionine) containing a Complete Protease Inhibitor Cocktail tablet (Roche). The homogenate was centrifuged at 13,400 *g* for 10 min at 4°C to separate the protein-containing intermediate layer from the lipid top layer and the cell-debris pellet. The protein suspension was stored at −80°C until use.

Proteins separated by gradient SDS-PAGE (4–12%) were transferred to a PVDF membrane using a Trans-Blot SD semi-dry blotting apparatus (Bio-Rad Laboratories, Hercules, CA, USA). The membrane was incubated for ∼45 min at room temperature (RT) in TBS + 1% dry-milk powder. The membrane was subsequently incubated at RT for 1 h in TBS+1% BSA containing first the α-HA antibody (Roche), and then the secondary antibody goat α-rat-IgG:HRP (Jackson). Bound horseradish peroxidase (HRP) was detected by chemiluminescence.

Statistics

Data are reported as means ± SEM. Means between groups of data were compared using one-factor analysis of variance (ANOVA), as well as paired or unpaired forms of the Student's *t* test (Microsoft Excel 2002). $P < 0.05$ is considered significant. Rates of pH_i recoveries were determined by linear fits to pH_i *vs.* time using a least-squares method with custom-designed software written by Mr Duncan Wong (Department of Cellular and Molecular Physiology, Yale University) for the W. F. Boron laboratory.

Results

Injection of PIP$_2$

Using the two-electrode voltage-clamp technique on whole oocytes, each expressing one of the three NBCe1 variants, we examined the effect of injecting PIP_2 on NBC-mediated, HCO_3^--induced outward currents. In an NBCe1-C-expressing oocyte clamped at −60 mV (Fig. 2*A*), briefly switching from the nominally CO_2/HCO_3^--free ND96 solution (pH 7.5) to one containing 5% CO_2–33 mM HCO_3^- (pH 7.5) elicited abrupt outward currents (Fig. 2*Aa* and *b*) due to the cotransport of Na^+, HCO_3^-, and net-negative charge into the oocyte. Injecting ∼50 nl of a 100 μM PIP_2 stock solution increases intracellular PIP_2 by an estimated 10 μM (an estimate based on an average oocyte volume of 1 μl and an aqueous compartment comprising 40% of the total volume; Zeuthen *et al.*, 2002). This injection elicited an inward 'sag' current (after arrow), which has previously been observed in oocytes injected with IP_3 (Oron *et al.* 1985). The IP_3-mediated 'sag' current arises from activation of Ca^{2+}-activated Cl^- channels (Yoshida & Plant, 1992) and can have two components: (i) a fast inward current due to ER Ca^{2+} release, and (ii) a slow inward current due to Ca^{2+} influx through SOCC activity. The magnitudes and time courses of these currents vary depending on factors including the depth and location of injection (Gillo *et al.* 1987; Lupu-Meiri *et al.* 1988). At 5 and 10 min after the PIP_2 injection, we assayed for NBC activity again by switching to the HCO_3^- solution, which elicited outward currents that were ∼2-fold larger (Fig. 2*Ac* and *d*). In most experiments, the injected PIP_2-stimulated, HCO_3^--induced outward current did not increase appreciably at 10 min. We use the term 'injected PIP_2' rather than 'PIP_2' because, as described in more detail below, injected PIP_2 stimulation is primarily indirect and operates through the IP_3/Ca^{2+} pathway. HCO_3^--induced currents were inhibited ∼80% by 200 μM of the HCO_3^--transport inhibitor DIDS (Fig. 2*Ae*), similar to that previously reported for NBCe1-A without PIP_2 injection (Liu *et al.* 2007. In four similar experiments, 4,4′-diisothiocyanatostilbene-2,2′-disulfonic acid (DIDS) inhibited the injected PIP_2-stimulated, HCO_3^--induced outward current by 82 ± 1%. The slight outward current elicited by applying DIDS in ND96 may be due to inhibition of either an anionic conductance or NBC activity due to residual intracellular HCO_3^-.

Using the same protocol as described for Fig. 2*A*, we performed two types of control experiments. In one set of control experiments, injecting H_2O instead of PIP_2 failed to stimulate NBCe1-C (Fig. 2*B*). Therefore, the injection procedure and associated cell swelling did not alter the NBC current in our assay. In the other set of control experiments, injecting PIP_2 into a H_2O-injected null oocyte (Fig. 2*C*) had little effect on the small endogenous HCO_3^--induced currents in our assay ($n = 4$).

Figure 2*A*-type experiments were also performed on oocytes expressing NBCe1-A and -B, and the summary data are shown in Fig. 2*D*. PIP_2 injection failed to stimulate the A variant (bar 1), but stimulated the B variant by ∼130% (bar 2) and the C variant by ∼110% (bar 3). As described below, the A variant is more active than the B and C variants expressed in oocytes. However, injected PIP_2 also failed to stimulate the A variant when we performed these experiments at a holding potential (−120 mV) where the A variant is less active (because of the reduced driving force favouring influx), but resembles the lower activity of the B and C variants (not shown). As described for Fig. 2*B*, injecting H_2O instead of PIP_2 failed to stimulate NBCe1-C activity (bar 4). We reasoned that the selective stimulation by PIP_2 injection of the B and C variants, but not the A variant is due to their common N terminus that differs in the A variant (Fig. 1). Indeed, as summarized by bar 5 in Fig. 2*D*, we found that injecting PIP_2 did not significantly stimulate an NBCe1-C construct with its N-terminal 87 residues deleted ($C_{\Delta N87}$)— a construct that our group has previously characterized (McAlear *et al.* 2006). Similar results were obtained with the corresponding N terminal

truncation of the B variant (data not shown). Therefore, stimulation by PIP_2 injection of the B and C variants requires their distinguishing N terminus.

In the absence of PIP_2 injection, the HCO_3^--induced outward currents are approximately 3- to 4-fold larger from the A *vs.* B and C variants, and ~3-fold larger for mutant $C_{\Delta N87}$ *vs.* wild-type C (McAlear *et al.* 2006). According to Fig. 2*D*, PIP_2 injection had little effect on the relatively large A-variant current, but approximately doubled the size of the B/C-variant currents. Thus, PIP_2 injection increased the B/C-variant currents to resemble those of $C_{\Delta N87}$ and the A variant more closely.

We next examined the effect of injecting PIP_2 on the voltage dependence of the three NBCe1 variants, as well as $C_{\Delta N87}$ (Fig. 3 and Supplemental Fig. 1). HCO_3^--dependent *I–V* plots were generated by subtracting plots obtained from oocytes bathed in ND96 from those bathed in the CO_2/HCO_3^- solution for 5 min (to allow for intracellular CO_2 to equilibrate). As expected, the injected PIP_2-stimulated, HCO_3^--dependent *I–V* plots in these experiments were largely inhibited by 200 μM DIDS (McAlear *et al.* 2006) as determined by switching back to ND96 briefly, applying DIDS, and then switching to the HCO_3^- solution for ~40 s. For NBCe1-A-expressing oocytes, the HCO_3^--dependent *I–V* plot was nearly linear and displayed slight outward rectification (Fig. 3*A*) as previously reported (Sciortino & Romero, 1999; McAlear *et al.* 2006). The *I–V* plot was minimally affected by injecting PIP_2, consistent with the summary data presented in Fig. 2*D*.

For both the C variant (Fig. 3*B*) and the B variant (Supplemental Fig. 1*A*), the near-linear shape of the HCO_3^--dependent *I–V* plots was similar to that of A, although the current magnitudes were less, as previously reported (McAlear *et al.* 2006). In contrast to that seen with the A variant, PIP_2 injection stimulated the HCO_3^--dependent outward currents of the B and C variants at V_m more positive than ~−100 mV. For the C-variant data, the mean *I–V* plots before and after

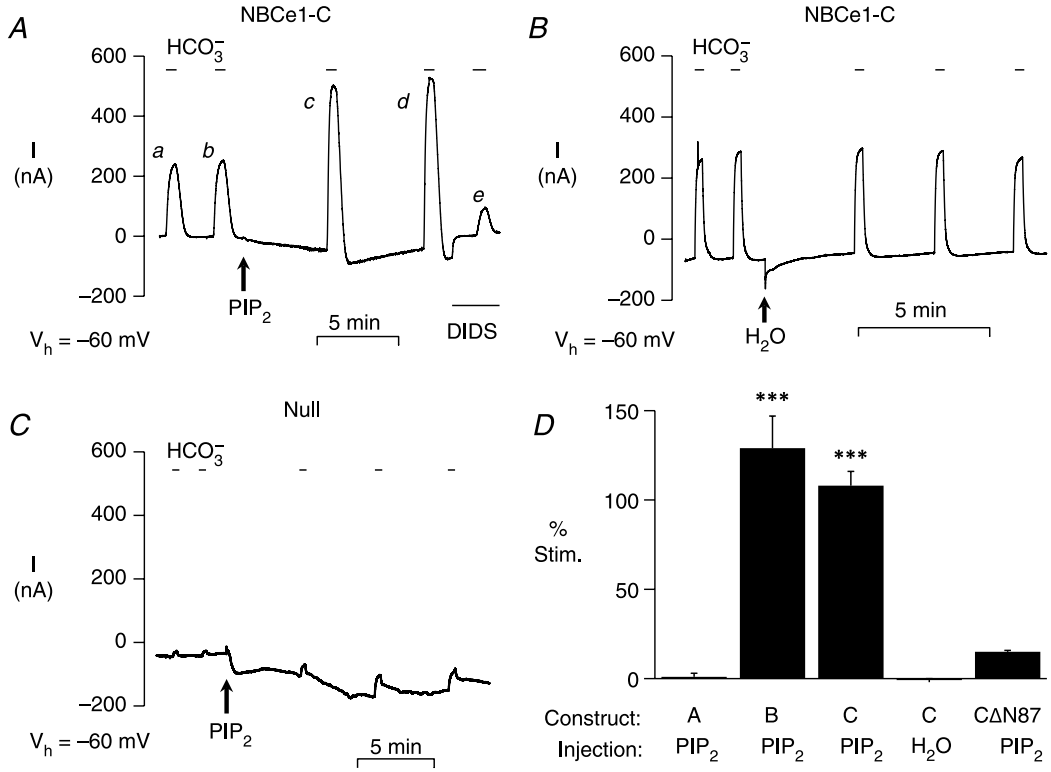

Figure 2. Injecting PIP_2 stimulates the HCO_3^--induced outward currents of the B and C variants
A, switching from ND96 to CO_2/HCO_3^- elicited NBC-mediated, HCO_3^--induced outward currents (*a* and *b*) in an NBCe1-C-expressing oocyte voltage clamped at −60 mV. Injecting 100 μM PIP_2 (~10 μM final concentration) increased the HCO_3^--induced outward currents ~2-fold (*c* and *d*), and these currents were inhibited ~80% by 200 μM DIDS (*e*). *B*, a similar experiment to that described in panel *A* was performed on an NBCe1-C-expressing oocyte, but H_2O instead of PIP_2 was injected. H_2O injection did not alter the HCO_3^--induced outward currents. *C*, in another control experiment on a H_2O-injected null oocyte, injecting PIP_2 did not appreciably stimulate endogenous HCO_3^--induced outward currents. *D*, summary data from panel *A*- and *B*-type experiments performed on all three variants, as well as a C variant missing its N-terminal 87 residues ($C_{\Delta N87}$). ***$P \leq 0.001$ for the mean current pre *vs.* post-injection. $n \geq 4$ for each bar.

$CO_2/HCO_3^- \pm PIP_2$ are shown in Supplemental Fig. 1*B* and *C*.

The apparent sigmoidal nature of the injected PIP_2-stimulated *I–V* profiles at positive potentials is most likely due to time-dependent changes in the HCO_3^--independent current after PIP_2 injection rather than a PIP_2-induced shift in the voltage dependence of the NBC. We determined the effect of injected PIP_2 on the NBC (HCO_3^--dependent) *I–V* relationship by subtracting the *I–V* plot in ND96 (5 min after injection) from that obtained from oocytes bathed in CO_2/HCO_3^- for 5 min (i.e., 10 min after injection). The assumption is that the HCO_3^--independent *I–V* plot will not change during those 5 min extra minutes to allow for CO_2/HCO_3^- to equilibrate— an assumption that is historically reasonable. However, in separate experiments, we found that the ND96 currents were smaller, but variable at 10 *vs.* 5 min after PIP_2 injection. The difference was particularly pronounced at the more positive potentials (Supplemental Fig. 1*D*). In principle, a correction factor from these separate experiments could be determined and used to scale the ND96 *I–V* plots in the other experiments designed to estimate PIP_2's effect on the NBC *I–V* relationship. However, there are limitations to the reliability of such a correction primarily because the mean correction factor is obtained from unpaired experiments with considerable variability. The mean correction factor may not match the true correction factor for a given NBC *I–V* plot experiment. Nevertheless, in using this correction-factor approach, we estimated a more linear NBC *I–V* relationship than shown in Fig. 3 at the more positive potentials.

Consistent with lost stimulation by PIP_2 injection of $C_{\Delta N87}$ shown in Fig. 2*D*, injecting PIP_2 failed to alter the HCO_3^--dependent *I–V* plot of $C_{\Delta N87}$ (Fig. 3*C*). H_2O-injected null oocytes did not exhibit

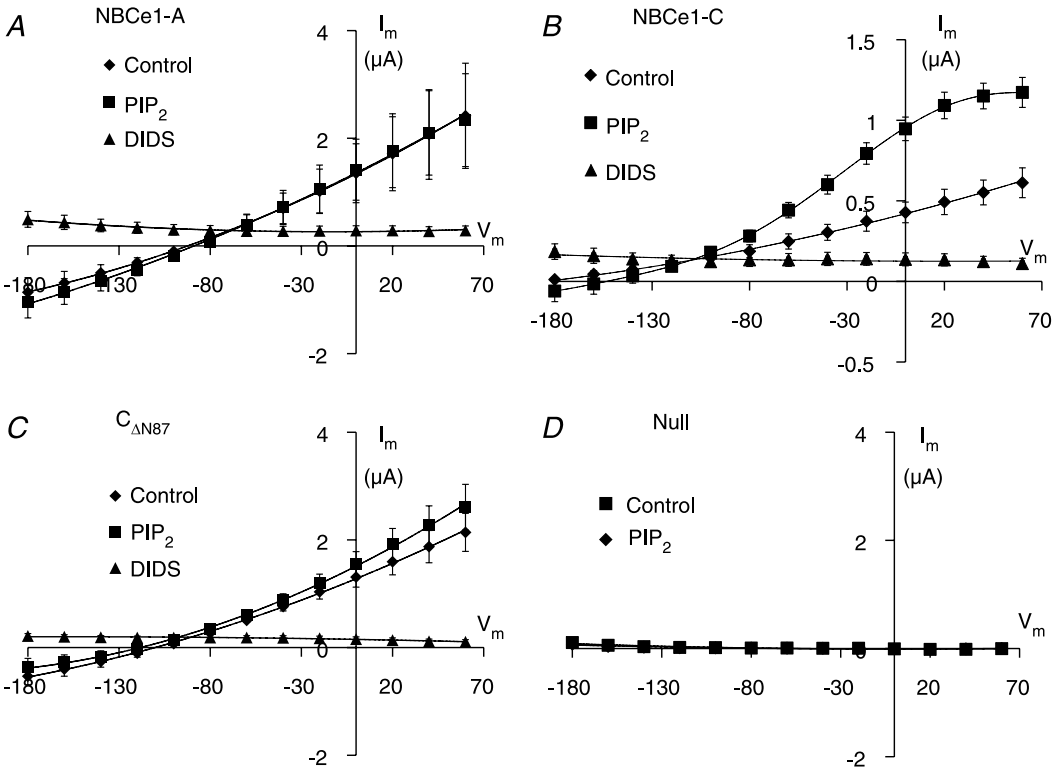

Figure 3. Injecting PIP_2 stimulates the voltage-dependent HCO_3^--induced currents of the B and C variants

A, the mean HCO_3^--dependent *I–V* plots from NBCe1-A-expressing oocytes were similar before injecting PIP_2 (diamonds) and after (squares). DIDS at 200 μM inhibited the currents (triangles). *B*, the mean HCO_3^--dependent currents from NBCe1-C-expressing oocytes at potentials more positive than ~ -100 mV were smaller before injecting PIP_2 (diamonds) than after (squares). DIDS at 200 μM inhibited the currents (triangles). *C*, the mean HCO_3^--dependent *I–V* plots for $C_{\Delta N87}$ were similar to those for the A variant (panel *A*). *D*, negligible currents were observed in H_2O-injected null oocytes. The upward-shifted *I–V* plots with DIDS in panels *A–C* presumably reflect different baseline currents inherent in these experiments designed to minimize the delay between HCO_3^--induced currents $\pm$ DIDS after PIP_2 injection. For each panel, $n = 3$ from 1 batch of oocytes, and the data were repeated in a second batch.

HCO_3^--dependent currents before or after PIP_2 injection (Fig. 3*D*). In summary, injecting PIP_2 stimulates the B and C variants (but not the A variant) in a broad range of membrane potentials.

Role of IP_3, PLC activity, and IRBIT

To determine the mechanism by which injecting PIP_2 stimulates NBCe1-B and -C, we tested the hypothesis that PIP_2 injected into oocytes is hydrolysed by constitutively active PLC to the signalling molecules IP_3 and diacylglycerol (DAG). Prior to the experimental trace shown in Fig. 4*A*, an NBCe1-C-expressing oocyte was preincubated for 40 min in ND96 containing 10 μM of the membrane permeant PLC inhibitor U73122. Subsequently, the oocyte was voltage-clamped at –60 mV and NBC activity was assayed as described for Fig. 2*A*. The NBC-mediated, HCO_3^--induced outward currents at the beginning of the experiment were only slightly larger after injecting PIP_2. Similar experiments were performed on the A and B variants, and the data are summarized in Fig. 4*B*. For each variant, we determined the percentage stimulation by PIP_2 injected into oocytes preincubated in either the inactive analogue U73343 (Fig. 4*B*, filled bars) or the active U73122 (Fig. 4*B*, open bars). The inactive analogue did not appreciably alter the mean percentage stimulation by injected PIP_2 (Fig. 4*B* *vs.* Fig. 2*D*). In contrast, the PLC inhibitor U73122 reduced the injected PIP_2-induced percentage stimulation by ~80% for the B and C variants. For the A variant, U73122 moderately increased the stimulation to ~30%. In the absence of PLC inhibition, PIP_2 injection did not stimulate the A variant presumably because the PIP_2 was rapidly hydrolysed. In summary, PIP_2 in the absence of hydrolysis (i.e., with U73122 pretreatment) significantly stimulated all three variants 20–30%— a finding that may reflect a direct stimulatory effect of PIP_2. As a control, H_2O injection did not stimulate the variants (Fig. 4*B*, hatched bars). In summary, stimulation of the B and C variants by PIP_2 injection requires PLC-mediated hydrolysis of PIP_2.

As described in Supplemental Fig. 2, U73122 pretreatment influences NBC surface expression and function independent of stimulation by PIP_2 injection. Specifically, U73122 pretreatment decreased the surface expression of the three variants by 30–60% based on SOC analysis (Supplemental Fig. 2*A*). Thus, constitutive PLC activity contributed to plasma-membrane expression of NBCe1. Regarding function, U73122 did not significantly alter the NBCe1-B/C current normalized to surface expression, but dramatically lowered the normalized NBCe1-A current by 80% (Supplemental Fig. 2*B*). Constitutive PLC activity is therefore required for the large A-variant currents.

The aforementioned U73122 data are consistent with PIP_2 hydrolysis to IP_3 and DAG being responsible for stimulation of the B and C variants. If IP_3 is responsible, then injecting IP_3 should mimic the stimulatory effect of injecting PIP_2. Using the experimental approached described for Fig. 2*A*, we found that injecting ~50 nl of a 100 μM IP_3 stock solution (which raised intracellular [IP_3] by an estimated 10 μM) stimulated the HCO_3^--induced current in an NBCe1-C-expressing oocyte by ~150% (Fig. 5*A*). The maximal IP_3-stimulated, HCO_3^--induced current was evident 5–15 min after injection. The IP_3 stimulation required extracellular Na^+ (data not shown) as expected for increased NBC activity. We performed similar experiments on the A and B variants, as well as

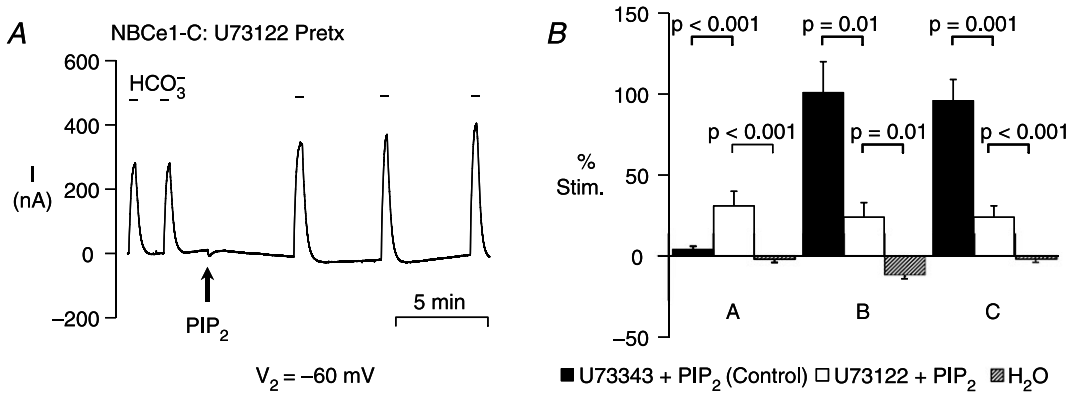

Figure 4. Full stimulation by PIP_2 injection of the B and C variants requires PLC activity
A, PIP_2 injection elicited only a modest stimulation of the HCO_3^--induced outward current in an oocyte pre-incubated for 30 min in 10 μM of the PLC inhibitor U73122. *B*, summary data of the mean injected PIP_2-induced percentage NBC stimulation from panel *A*-type experiments on the three variants. For oocytes pre-incubated in the inactive analogue U73343, subsequent PIP_2 injection had little effect on the A variant, but stimulated the B and C variants by ~100% (filled bars). Pre-incubating oocytes in U73122 reduced the stimulation by PIP_2 injection of the B and C variants to ~35%, and increased the stimulation of the A variant by the same extent (open bars). H_2O injection failed to stimulate any of the variants (hatched bars). $n \geq 3$ for each bar. Pretx, pretreatment.

$C_{\Delta N87}$, and present the summary data in Fig. 5*B*. The IP_3 stimulatory profile for the NBCs is identical to that for injected PIP_2 presented in Fig. 2*D*. More specifically, the IP_3 injection did not stimulate the A variant (Fig. 5*B*, bar 1), but stimulated the B variant by 190% (Fig. 5*B*, bar 2) and the C variant by ∼170% (Fig. 5*B*, bar 3). Finally, full IP_3 stimulation of the C variant requires the N terminus because the percent stimulation of $C_{\Delta N87}$ was only ∼50% (Fig. 5*B*, bar 4) compared to ∼170% for wild-type.

We also performed Fig. 5*A*-type experiments and injected IP_3 stock concentrations of 10 μM and 1 μM that are predicted to raise intracellular concentrations to more physiological levels of 1 μM and 100 nM, respectively. These experiments were performed in 0 Ca_o^{2+}, which does not affect NBC-mediated HCO_3^--induced currents (Supplemental Fig. 3*A*). As summarized in Fig. 5*C*, all three IP_3 concentrations stimulated NBCe1-C to the same extent. Thus, injecting an amount of IP_3 that raises the intracellular concentration by only 100 nM mimics the effect of injecting PIP_2. Also, the stimulation was similar to that seen for oocytes bathed in the presence of external Ca^{2+} (Fig. 5*B*). Thus, the IP_3 stimulation did not require an influx of Ca_o^{2+}, for example through SOCCs. In control experiments, injecting IP_3 did not markedly stimulate the small HCO_3^--induced currents in H_2O-injected null oocytes bathed either in the presence of Ca^{2+} (Supplemental Fig. 3*B*) or its absence (Supplemental Fig. 3*C*).

The NBCe1 variant-specific IP_3-induced stimulation parallels the findings of Shirakabe *et al.* (2006) who found that co-expressing the IP_3 receptor binding protein IRBIT stimulates the B variant (but not the A variant) in oocytes by binding to the N terminus. In similar experiments, IRBIT also stimulates NBCe1-C (Thornell *et al.* 2010; Yang *et al.* 2011). We considered the possibility that IP_3 injection in our experiments stimulates B/C by displacing endogenous IRBIT from its receptor. However, this possibility appears unlikely due to low expression levels of endogenous *vs.* exogenously expressed IRBIT in oocytes (Shirakabe *et al.* 2006). Using a more rigorous approach, we examined oocytes co-expressing NBCe1-C and the S68A mutant of IRBIT (Ando *et al.* 2006), which has

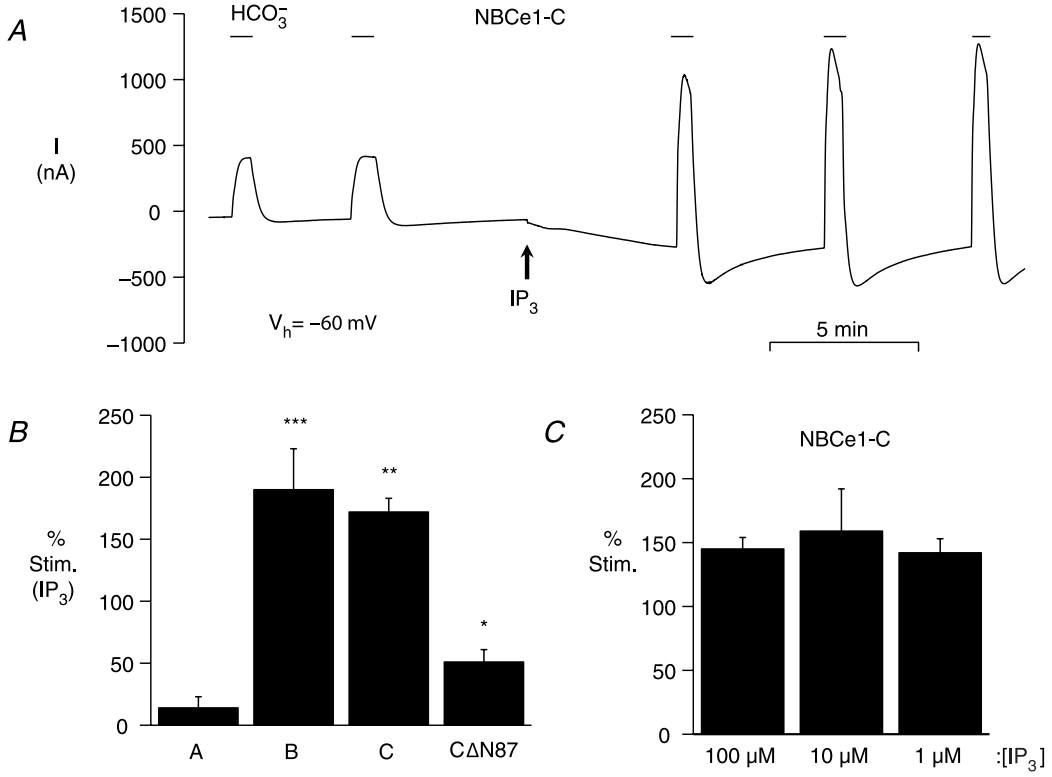

Figure 5. Injecting IP_3 —even at a low concentration— stimulates the HCO_3^--induced outward currents of the B and C variants
A, IP_3 injection stimulated the HCO_3^--induced outward currents by ∼3-fold in an NBCe1-C-expressing oocyte. *B*, summary data of the mean IP_3-induced percentage NBC stimulation from panel *A*-type experiments on the three variants, as well as $C_{\Delta N87}$. ***$P \leq 0.001$, **$P \leq 0.01$, and *$P \leq 0.05$ for the mean current pre- *vs.* post-injection. $n = 5$ for each bar. *C*, summary data of the mean IP_3-induced percentage NBC stimulation from panel *A*-type experiments on NBCe1-C-expressing oocytes injected with one of three different concentrations of IP_3. These experiments with different IP_3 injections were performed in Ca^{2+}-free solutions containing 1 mM EGTA. $n \geq 5$ for each bar.

previously been shown not to stimulate NBCe1-B activity (Shirakabe *et al.* 2006). This mutant only weakly binds to the IP_3 receptor because of the lost phosphorylation site. Furthermore, this mutant exerts a dominant-negative effect by multimerizing with wild-type IRBIT through interaction of the C-terminal tails independent of the aforementioned phosphorylation sites (Ando *et al.* 2006).

In the co-injected oocyte shown in Fig. 6*A*, the IP_3-stimulated HCO_3^--induced outward currents were similar to those seen in Fig. 5*A* without mutant IRBIT. We used immunoblot analysis to confirm NBCe1-C and S68A IRBIT co-expression in batch-matched oocytes. According to the summary data, the mean IP_3-stimulated, HCO_3^--induced current was unaffected by co-expressing S68A IRBIT (Fig. 6*B*). Thus, IP_3 stimulation of NBCe1-C does not involve IRBIT. As presented in Supplemental Fig. 4, similar results were obtained with an S71A mutant of IRBIT, which also only weakly binds to the IP_3 receptor because of the lost phosphorylation site (Ando *et al.* 2006), and probably also exerts a dominant-negative effect.

Role of Ca^{2+} and kinases

Because stimulation by PIP_2 injection of NBCe1 is blocked by a PLC inhibitor, and mimicked by IP_3 without a requirement for Ca_o^{2+}, we hypothesized that IP_3-mediated Ca^{2+} release from intracellular stores is necessary. If so, then ER Ca^{2+} depletion should block the PIP_2/IP_3 stimulation. To test this hypothesis, we depleted ER Ca^{2+} using a previously described protocol (Petersen & Berridge, 1994) in which oocytes were pretreated for 3–6 h in a modified Ca^{2+}-free ND96 solution containing 1 mM EGTA and 10 μM of the sarco/endoplasmic reticulum Ca^{2+}-ATPase (SERCA) inhibitor thapsigargin. The thapsigargin/0 Ca^{2+}-EGTA pretreatment did not affect surface expression of the NBCe1 variants (data not shown). Subsequently, oocytes were voltage-clamped at −60 mV and NBC activity assayed as described for Fig. 2*A* (i.e., in the presence of external Ca^{2+}, $[Ca_o^{2+}]$). After an NBCe1-C-expressing oocyte was pretreated with thapsigargin/0 Ca^{2+}-EGTA, PIP_2 injection actually inhibited rather than stimulated the HCO_3^--induced outward current (Fig. 7*A*). Similar experiments were performed on all three NBCe1 variants and $C_{\Delta N87}$, and the summary data are shown in Fig. 7*B*. The injected PIP_2-induced percentage stimulation of the B and C variants under control conditions with dimethyl sulphoxide (DMSO) pre-incubation (Fig. 7*B*, filled bars) was eliminated by the thapsigargin/0 Ca^{2+}-EGTA pretreatment (Fig. 7*B*, open bars). The stimulation by PIP_2 injection remained absent for the pretreated A variant and $C_{\Delta N87}$ mutant.

As shown in Fig. 7*C*, we replicated the experimental protocol on the C variant described in Fig. 7*A*, but injected IP_3 instead of PIP_2. The thapsigargin/0 Ca^{2+}-EGTA pretreatment inhibited IP_3-stimulated NBC activity, similar to that seen for injected PIP_2. According to the summary data of the tested variants, the percentage stimulation profiles were similar for injected PIP_2 (Fig. 7*B*) and IP_3 (Fig. 7*D*). Note that the small IP_3-induced percentage stimulation with $C_{\Delta N87}$ (also seen in Fig. 5*B*) was also inhibited by Ca^{2+}-store depletion. In summary, both injected PIP_2 and IP_3 stimulation of NBCe1-B/C require ER Ca^{2+} release.

We next tested the possibility that a rise in $[Ca^{2+}]_i$ independent of intracellular stores can stimulate the B and C variants. We took advantage of our thapsigargin/0 Ca^{2+}-EGTA protocol that depletes ER Ca^{2+} stores and in turn primes the activity of SOCCs in an attempt to replenish those stores. Thereafter, re-exposing an oocyte to Ca_o^{2+} triggers Ca^{2+} influx through the activated SOCCs (Petersen & Berridge, 1994). In the experiment

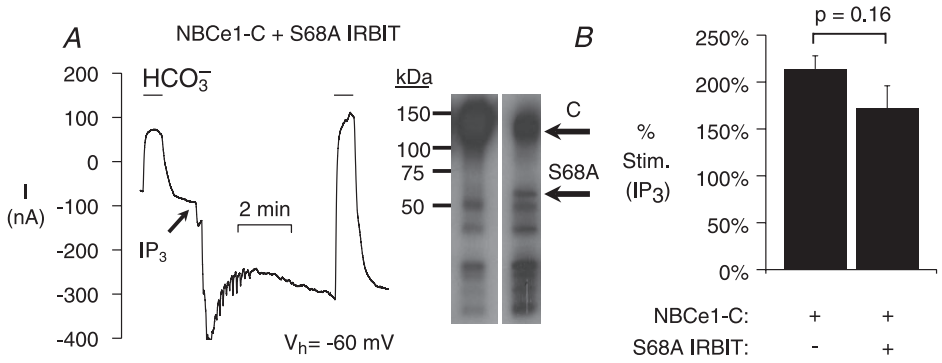

Figure 6. Co-expressing S68A IRBIT does not inhibit the IP_3-induced stimulation of NBCe1-C
A, as shown on the left, IP_3 injection stimulated the HCO_3^--induced outward current by ∼3-fold in an oocyte co-injected with equal amounts of NBCe1-C and S68A IRBIT cRNA. The break in the current trace at −400 nA denotes values below −400 nA not shown. As shown by an immunoblot on the right, an individual oocyte injected with NBCe1-C cRNA expressed ∼130 kDa NBCe1-C (left column), whereas an oocyte co-injected with both cRNAs expressed ∼130 kDa NBCe1-C and ∼60 kDa S68A IRBIT (right column). *B*, summary data of the mean IP_3-induced percentage NBC stimulation from panel *A*-type experiments on oocytes expressing NBCe1-C with or without S68A IRBIT ($n = 7$ for each bar).

shown in Fig. 8*A*, we pretreated the NBCe1-C-expressing oocyte in thapsigargin/0 Ca^{2+}-EGTA for 4–6 h, and then began the voltage-clamp experiment (−60 mV) with the oocyte still bathed in 0 Ca^{2+}-EGTA. The SERCA was still inhibited during the experiment because the effect of thapsigargin is irreversible. Note that the two NBC-mediated HCO_3^--induced outward currents in the continued absence of Ca_o^{2+} were small. Returning Ca_o^{2+} elicited a rapid, but transient inward current due to the influx of Ca^{2+} through the SOCCs stimulating Ca^{2+}-activated Cl^- channels. After returning the Ca_o^{2+}, the NBC-mediated, HCO_3^--induced outward currents were ∼3-fold larger than at the beginning of the experiment. Furthermore, the magnitude of those currents decreased ∼50% shortly after returning the oocyte to the 0 Ca^{2+}/EGTA solution— a result consistent with decreasing $[Ca^{2+}]_i$ inhibiting NBCe1-C again. Similar experiments were performed on all three NBCe1 variants and $C_{\Delta N87}$, and the summary data are shown in Fig. 8*B*. The percentage stimulation profile for the NBCs elicited by Ca^{2+} influx through activated SOCCs is nearly identical to that for IP_3 (Fig. 5*B*).

Using SOC analysis, we examined the possibility that Ca^{2+} stimulated the NBC current by increasing surface expression of the transporter. According to the summary data presented in Fig. 8*C*, returning Ca_o^{2+} in our SOCC-activation protocol had little effect on the A variant, and modestly decreased the surface expression of the B, C, and $C_{\Delta N87}$ variants by 15–20% (open bars) compared to control conditions (filled bars) in the continued absence of Ca_o^{2+}. Therefore, the percentage stimulation values for B, C, and $C_{\Delta N87}$ reported in Fig. 8*B* are actually underestimates because they are uncorrected for the modest decreases in surface expression. In summary, the Ca^{2+}-stimulatory effect is not due to an increase in NBC surface expression.

Using the non-specific kinase inhibitor staurosporine, we tested if the IP_3/Ca^{2+} stimulation of NBC activity

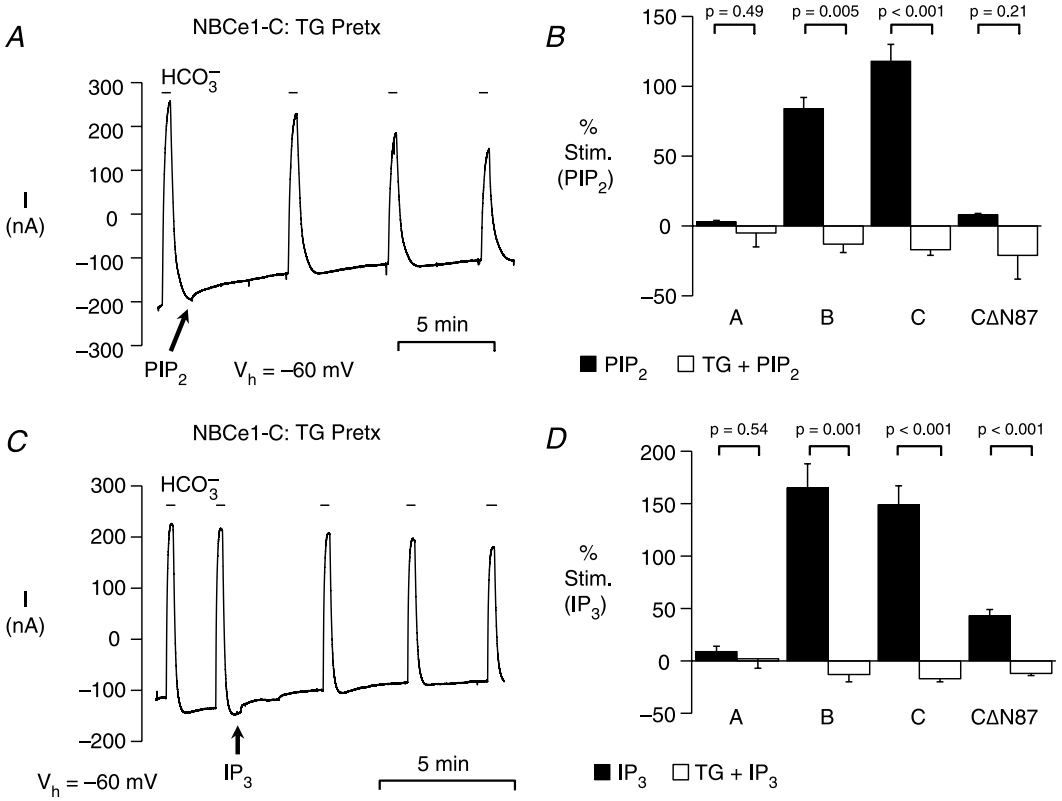

Figure 7. Depletion of ER Ca^{2+} blocks the injected PIP_2- and IP_3-stimulated HCO_3^--induced currents of the B and C variants

A, pre-incubating an NBCe1-C-expressing oocyte in a 0 Ca^{2+}/EGTA solution containing 10 μM thapsigargin (TG) for ∼4 h to deplete ER Ca^{2+} stores eliminated the injected-PIP_2 stimulation of the HCO_3^--induced outward current. *B*, summary data of the mean PIP_2-induced percentage NBC stimulation from panel *A*-type experiments on the three variants, as well as $C_{\Delta N87}$ with the oocytes pre-incubated in 0 Ca^{2+}/EGTA plus either DMSO (filled bars) or TG (open bars). $n \geq 3$ for each bar. *C*, the 0 Ca^{2+}/EGTA/TG pre-incubation also eliminated the injected-IP_3 stimulation of the HCO_3^--induced outward current of NBCe1-C. *D*, summary data of the mean IP_3-induced percentage NBC stimulation from panel *C*-type experiments on the variants with the oocytes pre-incubated in 0 Ca^{2+}/EGTA plus either DMSO (filled bars) or TG (open bars). $n \geq 3$ for each bar.

involves kinase activity. Prior to the experimental trace shown in Fig. 9*A*, an NBCe1-C-expressing oocyte was preincubated for 4 h in ND96 containing 20 μM staurosporine. The oocyte was then voltage-clamped at −60 mV, and NBC activity assayed as described for Fig. 2*A*. The NBC-mediated, HCO_3^--induced outward current at the beginning of the experiment was only slightly larger after injecting IP_3. According to the summary data

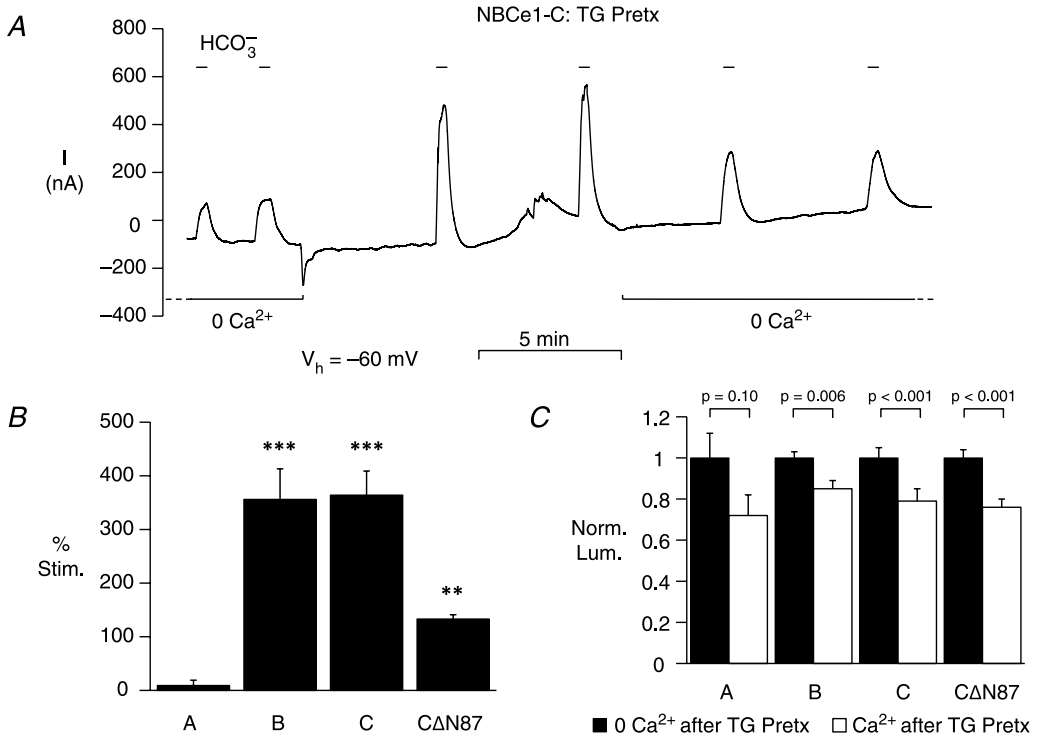

Figure 8. Activating store-operate Ca^{2+} channels stimulates the HCO_3^--induced outward currents of the B and C variants
A, the NBCe1-C-expressing oocyte was pre-incubated for ∼4 h in a 0 Ca^{2+}/EGTA solution containing 10 μM thapsigargin (TG) and maintained in the 0 Ca^{2+}/ETGA solution at the beginning of the experiment. Subsequently returning Ca_o^{2+} stimulated the HCO_3^--induced outward currents by ∼3-fold compared to the currents in the absence of Ca_o^{2+}. These stimulated currents were reversed by removing Ca_o^{2+}. *B*, summary data of the mean percentage NBC stimulation from panel *A*-type experiments on the three variants, as well as $C_{\Delta N87}$. $^{***}P \leq 0.001$ and $^{**}P \leq 0.01$ for the mean current pre- *vs*. post-injection. $n \geq 3$ for each bar. *C*, summary of mean single-oocyte chemiluminescence (SOC) from oocytes first pretreated with the 0 Ca^{2+}/EGTA/TG solution, and then either maintained in 0 Ca^{2+} (filled bars) or re-exposed to Ca_o^{2+} for 5 min (open bars). $n \geq 20$ (2 oocyte batches) for each bar.

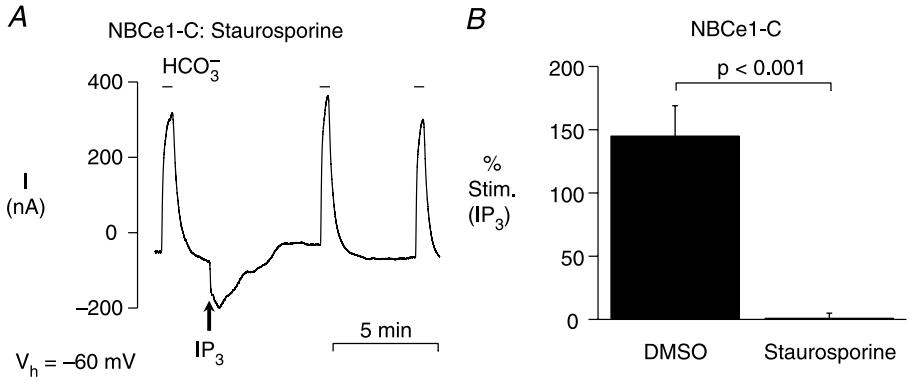

Figure 9. Staurosporine blocks the IP_3-induced stimulation of NBCe1-C
A, pre-incubating an NBCe1-C-expressing oocyte in ND96 containing 20 μM staurosporine for ∼4 h to inhibit kinase activity eliminated the injected-IP_3 stimulation of the HCO_3^--induced outward current. *B*, summary data of the mean IP_3-induced percentage NBC stimulation from panel *A*-type experiments from oocytes pretreated with DMSO (filled bar) or staurosporine (open bar). $n \geq 5$ for each bar.

(Fig. 9*B*), pretreating with staurosporine eliminated the IP_3-induced percentage stimulation (open bar) compared to pretreating with the vehicle DMSO (filled bar). Thus, the IP_3/Ca^{2+} stimulation of NBCe1-B/C requires activity of one or more kinases.

Endogenous activation of a G-protein coupled receptor (GPCR)

According to our injection experiments, PIP_2 stimulates NBCe1-B and NBCe1-C through PLC-mediated hydrolysis to IP_3 and subsequent release of ER Ca^{2+}. We next used a less invasive approach to hydrolyse PIP_2 to IP_3 by applying LPA to activate the endogenous GPCR in the oocyte (Durieux *et al.* 1992).

For the experiment on an NBCe1-C-expressing oocyte shown in Fig. 10*A*, we used the same experimental protocol as described above (e.g., Fig. 2*A*), except that solutions were Ca^{2+} free and contained EGTA. At the beginning of the experiment, NBC-mediated, HCO_3^--induced outward currents were ~200 nA. Subsequently applying 1 μM LPA for ~15 s elicited the sag current consistent with IP_3-mediated Ca^{2+} release and Ca^{2+}-activated Cl^- channel activity. This transient LPA exposure stimulated the HCO_3^--induced outward currents by ~150%, similar to that observed with PIP_2 injection (Fig. 2*A*). Applying LPA to a control (null) oocyte did not elicit appreciable HCO_3^--induced currents (Supplemental Fig. 5*A*).

If the LPA-induced NBC stimulation involves IP_3-mediated ER Ca^{2+} release, then chelating Ca_i^{2+} with BAPTA should inhibit the stimulation. Pre-incubating NBC-expressing oocytes for ~5 h in ND96 containing 10 μM BAPTA-AM had no effect on the surface expression of the variants (Supplemental Fig. 5*B*), but caused a modest decrease (~35%) in the HCO_3^--induced currents for the B and C variants (Fig. 10*B*). This decrease may reflect sensitivity of the B and C variants to baseline $[Ca^{2+}]_i$.

BAPTA pretreatment had a large inhibitory effect on the LPA-induced stimulation of NBCe1-C. As shown in Fig. 10*C*, pretreating with BAPTA dramatically reduced the LPA-induced stimulation of the HCO_3^--induced current compared to Fig. 10*A*. Note that BAPTA pretreatment also eliminated the LPA-induced inward sag current attributed to Ca^{2+}-activated Cl^- channel activity.

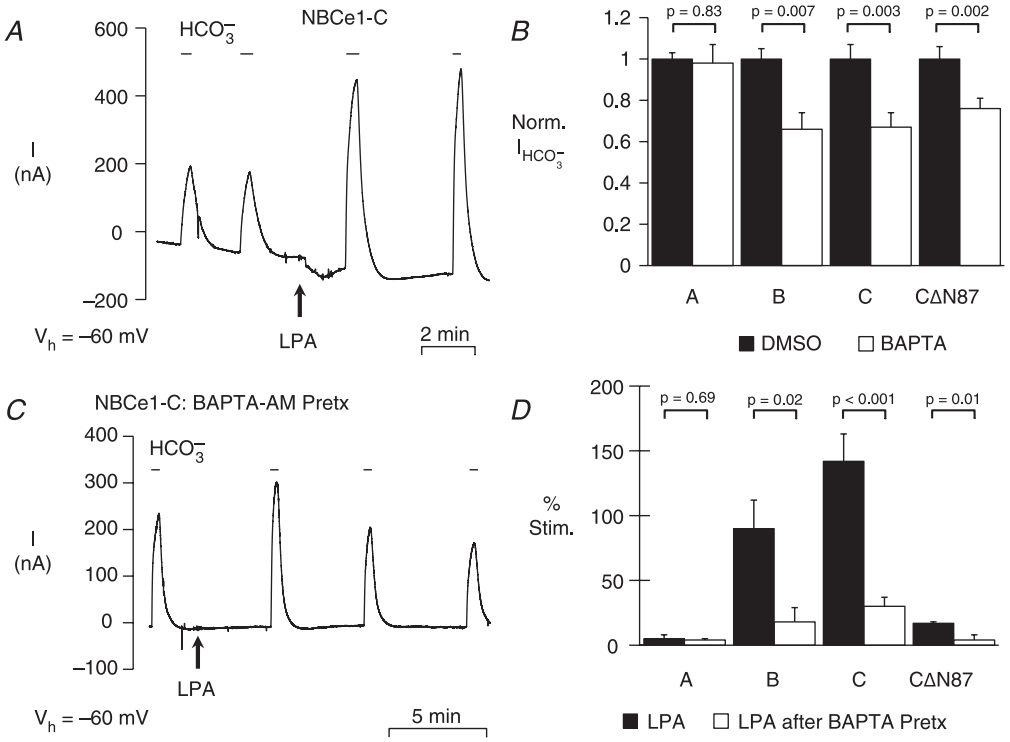

Figure 10. Lysophosphatidic acid (LPA) stimulates the HCO_3^--induced outward currents of the B and C variants
A, transiently exposing an NBCe1-C-expressing oocyte to 1 μM LPA for ~15 s stimulated the HCO_3^--induced outward currents by ~2.3-fold. *B*, summary data of the normalized HCO_3^--induced outward currents for variant-expressing oocytes pre-incubated for 5–7 h in DMSO (filled bars) *vs.* 10 μM BAPTA-AM (open bars). $n \geq 4$ for each bar. *C*, BAPTA-AM pre-incubation inhibited the LPA-stimulated, HCO_3^--induced currents in an NBCe1-C-expressing oocyte. *D*, summary data of the mean LPA-induced percentage NBC stimulation from panel *A*-type experiments on oocytes pretreated with DMSO (filled bars) or BAPTA-AM (open bars). $n \geq 4$ for each bar.

Similar Fig. 10*A*- and Fig. 10*C*-type experiments were performed on all three NBCe1 variants and $C_{\Delta N87}$, and the summary data are shown in Fig. 10*D*. LPA increased the HCO_3^--induced currents of the B and C variants, but not the A variant ($P = 0.30$) or $C_{\Delta N87}$ ($P = 0.10$) (filled bars). BAPTA pretreatment reduced the LPA-stimulated currents from 90% to ~20% for the B variant, and ~140% to 30% for the C variant (open bars).

We examined the effect of LPA on NBC surface expression. As summarized in Supplemental Fig. 5*C*, transient LPA application increased surface expression (after 5 min) of NBCe1-B, but not the other variants, with or without pretreatment with BAPTA. The LPA-induced increase in surface expression of the B variant accounts for the majority of the stimulated current. In summary, transient LPA application increases the NBCe1-B current predominantly by increasing NBC surface expression through a Ca^{2+}-independent mechanism. In contrast, LPA increases the NBCe1-C current by stimulating transporter activity through a Ca^{2+}-dependent mechanism.

We have examined the effect of LPA not only on the electrogenicity of NBCe1, but also on HCO_3^- transport and associated mediated changes in pH_i. In the oocyte experiments presented in Fig. 11,

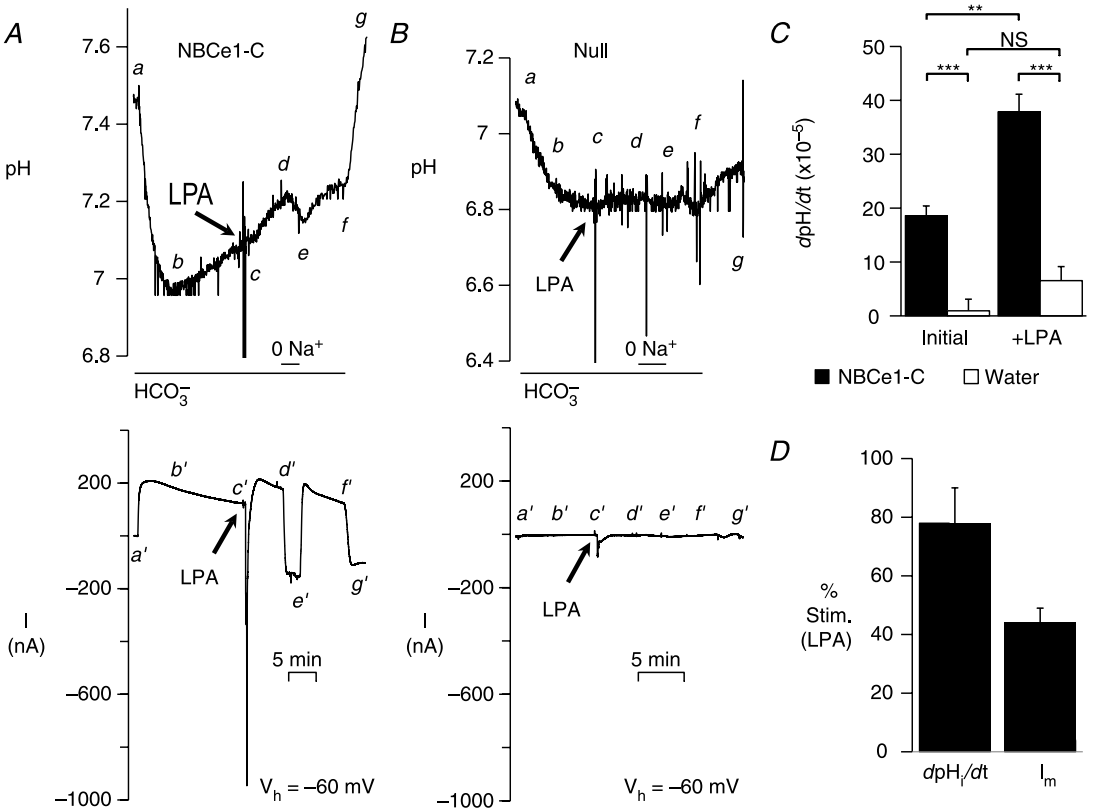

Figure 11. LPA stimulates both a HCO_3^--dependent pH_i recovery and outward current in an NBCe1-C-expressing oocyte voltage clamped at −60 mV
A, as shown in the top panel, switching from ND96 to CO_2/HCO_3^- elicited a pH_i decrease (*a*–*b*) due to CO_2 influx, followed by a recovery (*b*–*c*) due to NBC activity. Applying 1 μM LPA for ~15 s increased the pH_i recovery rate shortly thereafter (*c*–*d*) consistent with NBC stimulation. Removing and returning external Na^+ caused pH_i to decrease and then increase again (*d*–*e*–*f*). Switching back to ND96 caused pH_i to increase (*f*–*g*). In the simultaneous current recording, the HCO_3^- solution elicited the characteristic NBC-mediated outward current (*a*′–*b*′–*c*′). LPA induced a transient inward current presumably due to Ca^{2+}-activated Cl^- channel activity, followed by a pronounced outward current (*c*′–*d*′) due to NBC stimulation. Removing and returning external Na^+ reversed and then reinstated the outward current (*d*′–*e*′ –*f*′). Switching back to ND96 eliminated the outward current (*f*′–*g*′). *B*, a similar experiment was performed on a H_2O-injected null oocyte. As shown in the upper panel, the CO_2/HCO_3^- solution elicited the expected decrease in pH_i (*a*–*b*), but no subsequent pH_i recovery (*b*–*c*). Subsequent experimental manoeuvres had little effect on pH_i (*c*–*f*). As shown in the lower panel, the solutions had little effect on current (*a*′–*g*′). *C*, left pair of bars summarizes the mean dpH_i/dt from segment *b*–*c* pH_i recoveries for oocytes expressing NBCe1-C (filled bar) or injected with H_2O (open bar). Right pair of bars summarizes the mean dpH_i/dt obtained 5 min after applying LPA to oocytes expressing NBCe1-C (filled bar) or injected with H_2O (open bar). $n \geq 4$ for each bar. ***$P < .001$, **$P < .01$, NS = not significant. *D*, LPA stimulated the NBCe1-C-mediated dpH_i/dt (calculated from panel *C* data) by ~80% and current by ~40%. The downward pH_i spikes elicited by LPA in panels A and B are truncated at the lowest pH_i shown on each y-axis.

we simultaneously measured pH_i using ion-sensitive microelectrodes (upper panels) and currents with the voltage-clamp technique (lower panels). For a voltage-clamped NBCe1-C-expressing oocyte (Fig. 11*A*), switching from ND96 to the CO_2/HCO_3^- solution elicited an initial pH_i decrease due to the influx of CO_2 and subsequent hydration to HCO_3^- and H^+ (*a*–*b*). The HCO_3^- solution elicited the expected NBC-mediated outward current (*a*′–*b*′). After the initial decrease, pH_i slowly increased (*b*–*c*) due to NBC-mediated HCO_3^- entry, and the continual outward current slowly diminished (*b*′–*c*′). Applying 1 μM LPA increased the rate of the pH_i recovery (*c*–*d*) consistent with stimulation of NBC-mediated HCO_3^- transport. LPA generated a large, transient inward current—presumably due to IP_3/Ca^{2+}-stimulated Cl^- channels—followed by a larger outward current (*c*′–*d*′). The LPA-stimulated pH_i recovery rate and larger outward current were both consistent with increased NBC activity because removing external Na^+ (i) blocked the pH_i recovery and caused the pH_i to decrease (*d*–*e*), and (ii) reversed the outward current to an inward current (*d*′–*e*′). Returning external Na^+ reinstated the pH_i recovery (*e*–*f*) and outward current (*e*′–*f*′). Finally, switching back to ND96 caused pH_i to increase and overshoot the initial pH_i (*f*–*g*); the current also returned close to baseline (*f*′–*g*′).

A similar experiment was performed on a null control H_2O-injected oocyte (Fig. 11*B*). As shown in the upper panel, the CO_2/HCO_3^- solution elicited the CO_2-induced pH_i decrease (*a*–*b*), but no subsequent pH_i recovery (*b*–*c*). The experimental manoeuvres of applying LPA (*c*–*d*), as well as removing and returning external Na^+ (*d*–*e*–*f*) had little effect on pH_i. All the aforementioned manoeuvres did not elicit appreciable changes in current (lower panel).

From experiments similar to those presented in Fig. 11*A* and *B*, we calculated the mean dpH_i/dt during the initial segment *b*–*c* pH_i recovery (left pair of bars, Fig. 11*C*) for NBCe1-C-expressing oocytes (filled bars) and control oocytes (open bars). As expected, NBC-expressing oocytes displayed a HCO_3^--induced pH_i recovery rate greater than that seen in control oocytes. We also computed the mean LPA-stimulated dpH_i/dt (right pair of bars) for NBCe1-C-expressing oocytes (filled bars) and control oocytes (open bars) at the 5 min time point after applying LPA (to match LPA-stimulated NBC current measurements in the previous voltage-clamp experiments). The pH_i recovery rate was markedly greater in NBCe1-C-expressing oocytes exposed to LPA. Using the dpH_i/dt data from NBCe1-C-expressing oocytes in Fig. 11*C*, we subtracted the corresponding mean dpH_i/dt values from water-injected oocytes to calculate that LPA stimulated the NBCe1-C-mediated dpH_i/dt by ∼80% (Fig. 11*D*). To analyze the current data, we determined the LPA-stimulated current at the 5-min time point relative to the current immediately before applying LPA (point *c*′) after subtracting the corresponding currents from water-injected oocytes. LPA stimulated the NBCe1-C-mediated current by ∼40%.

Discussion

Stimulation by PIP$_2$ injection of the B and C variants, but not the A variant, of NBCe1

Our main conclusion is that PIP_2 injection stimulates the B and C variants —but not the A variant— expressed in oocytes through the classic IP_3/Ca^{2+} pathway that involves at least one staurosporine-sensitive protein kinase. There are six observations that support this conclusion. First, the PLC inhibitor U73122 eliminates the stimulation by PIP_2 injection (Fig. 4). Second, injecting IP_3 mimics the stimulation by PIP_2 injection (Fig. 5). Third, depleting ER Ca^{2+} eliminates both the injected-PIP_2 and -IP_3 stimulation (Fig. 7). Fourth, raising $[Ca^{2+}]_i$ by activating SOCCs mimics the PIP_2/IP_3 stimulation, and to a greater extent (Fig. 8). Fifth, applying LPA to activate the endogenous GPCR in oocytes resembles PIP_2/IP_3 in stimulating the C variant in a Ca^{2+}-dependent manner (Fig. 10), and also increases the pH_i recovery rate from a CO_2-induced acid load (Fig. 11). Sixth, pretreating with staurosporine eliminates the IP_3 stimulation (Fig. 9).

The aforementioned observations are consistent with injected PIP_2 being hydrolyzed to intracellular IP_3 by basal PLC activity in oocytes. In addition, the following two NBC-independent observations provide further evidence for such hydrolysis. First, injecting PIP_2 (Fig. 2*A*), but not water (Fig. 2*B*), triggered a prolonged IP_3-mediated, Ca^{2+}-activated Cl^- current (sag current) similar to that previously reported in oocytes (Oron *et al.* 1985; Yoshida & Plant, 1992). Second, the PLC inhibitor U73122 greatly inhibited this sag current (Fig. 4*A*).

The mechanism by which IP_3-mediated Ca^{2+} release stimulates the B and C variants is not entirely clear. Regarding Ca^{2+}, Müller-Berger *et al.* (2001) in a related study used the inside-out macropatch technique to characterize the activity of rat-kidney NBCe1-A expressed in oocytes. They reported that raising bath (cytosolic) Ca^{2+} from 100 nM to 500 nM stimulated the NBC current in most patches by increasing the Na^+:HCO_3^- stoichiometry from 1:2 to 1:3. Although $PIP_2/IP_3/Ca^{2+}$ did not stimulate NBCe1-A in our study, injecting PIP_2 did elicit an apparent rightward shift of the HCO_3^--dependent reversal potential (E_{rev}) for oocytes expressing the B and C variants (e.g., Fig. 3). However, the observed E_{rev} shifts appear too small to result from an increase in transporter stoichiometry. There are other possible explanations, including a smaller HCO_3^- transmembrane gradient generated by a stimulated NBC that raises the HCO_3^- concentration on the inner surface of the membrane. Further studies are required

to assess any IP_3/Ca^{2+}-mediated change in transporter stoichiometry.

IP_3/Ca^{2+} stimulation of NBCe1 variants may account for GPCR activation of NBCe1. For example, Perry *et al.* (2006) working on oocytes heterologously expressing NBCe1-A and the Ang-II receptor AT_{1B} reported that low concentrations of Ang II caused a modest (i.e., 20–30%) stimulation of the HCO_3^--induced current that is Ca^{2+} dependent and perhaps partially inhibited by a PKC inhibitor. In our study, however, the B and C variants —not the A variant— were stimulated by IP_3/Ca^{2+}. Furthermore, as described in more detail below, this stimulation is independent of PKC. Perhaps other components of receptor activation direct cell signalling to a specific NBC variant.

The mechanism by which IP_3-mediated Ca^{2+} release stimulates the B and C variants involves a staurosporine-sensitive kinase. Müller-Berger *et al.* (2001) hypothesized that kinase activation is responsible for Ca^{2+} stimulation of NBCe1-A in the macropatch. Our data support this hypothesis for the B and C variants. The general kinase inhibitor staurosporine blocks the IP_3 stimulation of the C variant. However, some of the more well-known kinases do not seem to be involved. In Fig. 9-type experiments (not shown), IP_3 stimulation of NBCe1-C was unaffected by the PKC inhibitors PKC (17–31) and GF109203X, a calmodulin inhibitory peptide, or the DAG kinase inhibitor R59949. Further studies are required to identify the specific kinase(s) responsible.

Requirement of the N terminus for full IP_3/Ca^{2+} stimulation of NBCe1-B/C

The B and C variants share the same N terminus that differs in the A variant (Fig. 1). We therefore hypothesized that the different N terminus of B and C is required for full IP_3/Ca^{2+} stimulation. Indeed, the $PIP_2/IP_3/Ca^{2+}$ stimulation of a truncated NBCe1-C ($C_{\Delta N87}$) missing its 87 N-terminal residues was either eliminated or greatly inhibited. For example, injecting PIP_2 (Fig. 2) or applying LPA (Fig. 10) failed to stimulate $C_{\Delta N87}$. Furthermore, injecting IP_3 stimulated $C_{\Delta N87}$ by only 51% compared to 172% for wild-type C (Fig. 5*B*), and activating SOCCs stimulated $C_{\Delta N87}$ by only 133% compared to 364% for wild-type C (Fig. 8*B*). While the N terminus of B/C plays a major role in Ca^{2+} stimulation and a kinase is involved, the exact mechanism is not clear. Ca^{2+}-kinase stimulation presumably involves phosphorylation of either NBC itself or an associated protein. Such phosphorylation may remove the autoinhibitory domain (AID), either by targeting the AID itself within the N terminus, or the AID binding site elsewhere on the molecule. However, there may also be Ca^{2+}/kinase-sensitive regulation of NBCe1-B/C independent of the N terminus based on the findings that both IP_3 injection and SOCC activation modestly stimulated $C_{\Delta N87}$. Such stimulation was not seen with the A variant, perhaps due its different N terminus. Although there was some variability, $PIP_2/IP_3/Ca^{2+}$ stimulated the B and C variants in a similar degree. Furthermore, $PIP_2/IP_3/Ca^{2+}$ stimulated the A, but not B variant even though both have the same C terminus. Therefore, the different C termini of NBCe1 do not appear to contribute substantially to this mode of regulation.

IP_3/Ca^{2+}-mediated changes in surface expression

According to Fig. 8, our SOCC activation protocol, which promotes Ca^{2+} influx, stimulates the B and C variants even with a 15–20% decrease in surface expression (Fig. 8*C*). There is precedence for Ca^{2+}-activated internalization of NBCe1. For example, Perry *et al.* (2006, 2007) working on oocytes co-expressing NBCe1-A and the Ang-II receptor AT_{1B} reported that a high concentration of Ang II elicited a decreased in NBC activity due to PKC and Ca^{2+}-dependent internalization of the protein. However, we did not observe any $PIP_2/IP_3/Ca^{2+}$- or LPA-stimulated decrease in surface expression of the A variant. Furthermore, PKC inhibitors in our study did not inhibit the IP_3-mediated stimulation of the B and C variants (data not shown). Apparently, the effect of Ca^{2+} on NBCe1 expression is dependent on the NBCe1 variant studied and the receptor-signalling pathway activated. In fact, according to Supplemental Fig. 2, inhibiting basal PLC activity independent of receptor activation reduces surface expression and associated activity of NBCe1-A.

A curious finding in our study was the disparate mechanisms responsible for the LPA stimulation of the B *vs.* C variants. Although LPA stimulated the activity of both variants by at least 90% in a Ca^{2+}-dependent manner, the stimulation of the B but not the C variant was mainly attributed to an increase in surface expression (Supplemental Fig. 5*C*). Interestingly, the increase in NBCe1-B surface expression was not Ca^{2+} dependent (i.e., not inhibited by BAPTA) (Fig. 10*D*). The simplest interpretation is that the LPA-induced increase in NBCe1-B surface expression does not require elevated $[Ca^{2+}]_i$, although the associated increase in transporter activity does. Apparently, GPCR activation can influence the activity and expression of NBCe1 variants.

IP_3/Ca^{2+} stimulation independent of IRBIT

As described in the Introduction, IRBIT binds to the N terminus and stimulates the B but not A variant (Shirakabe *et al.* 2006) by removing the AID as proposed

by the authors. Furthermore, IRBIT also stimulates the C variant (Thornell *et al.* 2010; Yang *et al.* 2011). The PIP$_2$/IP$_3$/Ca^{2+} stimulatory effect on the B and C variants, but not the A variant, reported in this study is consistent with IRBIT's stimulatory profile. However, we believe that the PIP$_2$/IP$_3$/Ca^{2+} and IRBIT stimulatory pathways are distinct for the following four reasons. First, relative to heterologous expression, endogenous expression of IRBIT is low in oocytes (Shirakabe *et al.* 2006). Second, injecting IP$_3$ into ER Ca^{2+}-depleted oocytes that are returned to bath Ca^{2+} failed to stimulate NBCe1-B/C (Fig. 7). In these experiments, primed SOCC activity would provide sufficient cytosolic Ca^{2+} for IP$_3$-displaced IRBIT activity. Third, IP$_3$ stimulation of NBCe1-C is not abolished by a Ca^{2+}/calmodulin kinase inhibitor (data not shown). Ca^{2+}/calmodulin-mediated phosphorylation is required for IRBIT activity (Ando *et al.* 2006). Fourth, and most convincingly, co-expressing either the dominant-negative S68A IRBIT mutant (Fig. 6) or the less-characterized S71A IRBIT mutant (Supplemental Fig. 4) inhibits neither the HCO_3^--induced NBCe1-C current (which reinforces the first point above) nor its IP$_3$ stimulation. However, this fourth point relies on the following two assumptions: (i) exogenous human IRBIT multimerizes with any endogenous *Xenopus* IRBIT, and (ii) the dominant-negative nature of S68A IRBIT characterized in IP$_3$-receptor binding and Ca^{2+}-response studies (Ando *et al.* 2006) would extend to IRBIT stimulation of NBCe1.

Although the IP$_3$/Ca^{2+} and IRBIT stimulatory pathways are distinct, there may be some crosstalk. In oocytes expressing NBCe1-B/C, co-expressing IRBIT markedly inhibited the PIP$_2$-induced stimulation of the HCO_3^--induced NBC current (Thornell *et al.* 2010). However, we cannot exclude the possibility that elevated expression of IRBIT competes with injected PIP$_2$-generated IP$_3$ for the IP$_3$ receptor, thereby reducing Ca^{2+} release and NBC stimulation.

Physiological significance of PIP$_2$/IP$_3$/Ca^{2+} regulation of NBCe1-B/C activity

Our finding that PIP$_2$ stimulates NBCe1 activity through hydrolysis to IP$_3$ and subsequent ER Ca^{2+} release may have important implications for understanding receptor-mediated effects on acid–base transporter activity and pH$_i$ regulation, as well as functional coupling to Ca_i^{2+} physiology in tissues such as heart and brain. In brain, glutamate-induced metabotropic receptor activation and subsequent IP$_3$/Ca^{2+}-stimulated NBCe1 activity in glial cells would be expected to dampen extracellular alkaline shifts or augment acid shifts associated with neuronal activity (Chesler, 2003). PIP$_2$ regulation of NBCe1 activity may also contribute to important secretory or reabsorptive processes of epithelia. In the pancreas for example, secretin acting through an increase in cAMP is the primary stimulator of HCO_3^- secretion. However, other synergistic mechanisms appear to be involved as reviewed by Lee *et al.* (2012). IP$_3$/Ca^{2+} induced stimulation of NBCe1-B on the basolateral membrane may be responsible for additional PLC-mediated cholingeric and CCK$_A$ stimulation of ductal HCO_3^- secretion.

PIP$_2$ regulation of NBCe1 activity by a dual mechanism

The effect of PIP$_2$ on NBCe1 activity in oocytes is complex and appears to involve dual pathways based on results presented here and in our previous publication (Wu *et al.* 2009*b*). In the current study, we report that injecting PIP$_2$ into an intact oocyte heterologously expressing NBCe1 stimulates transporter current. The injected-PIP$_2$ stimulation is indirect and requires hydrolysis to IP$_3$, ER Ca^{2+}, and one or more kinases. Furthermore, this effect is variant specific and seen with the B and C variants, but not the A variant— a finding that supports the hypothesis that different bicarbonate transporter variants have different modes of regulation. This IP$_3$/Ca^{2+} regulation requires the 85 N-terminal residues of the B/C variants for full stimulation.

However, in a previous study, our group found that PIP$_2$ directly stimulates NBCe1 activity and reduces the rate of transporter rundown in excised patches from oocytes expressing the A variant (Wu *et al.* 2009*b*). Data presented in the current study also provide support for direct PIP$_2$ stimulation of expressed NBCe1 variants in whole oocytes. More specifically, in the presence of PLC inhibition, injecting PIP$_2$ stimulated all three variants —including the A variant— by 20–30% (Fig. 4*B*). However, we cannot exclude the possibility that residue PLC activity is responsible for the small stimulation of the B/C variants, although this possibility does not explain the stimulation of the A variant that is insensitive to PIP$_2$/IP$_3$ injection. Also, indirect effects of altering PIP$_2$ metabolism by PLC inhibition may be responsible. Finally, according to our recent preliminary data (not shown) on oocytes, activating a heterologously expressed voltage-sensitive phosphatase to reduce PIP$_2$ levels without IP$_3$ production inhibited NBCe1-C activity. Thus, it appears that PIP$_2$ itself is required for NBCe1 activity, and depleting PIP$_2$ independent of the IP$_3$/Ca^{2+} pathway reduces activity.

We are currently characterizing PIP$_2$ regulation of all NBCe1 variants at both the functional and molecular levels to understand if/how these two pathways regulate variant-specific NBCe1 activity either in concert or differentially. The dominance of one pathway over another may depend not only on the NBCe1 variant and its apparent PIP$_2$ affinity, but also on PIP$_2$ concentration,

particular signalling pathways, and perhaps PIP_2 microdomains or lipid rafts (Gamper & Shapiro, 2007). Physiologically, PIP_2 regulation of NBCe1 activity may explain pH changes linked to GPCR activation and PLC-mediated cellular processes as described above, as well as pathological conditions leading to ATP deficiency and associated PIP_2 degradation.

References

Abuladze N, Song M, Pushkin A, Newman D, Lee I, Nicholas S & Kurtz I (2000). Structural organization of the human NBC1 gene: kNBC1 is transcribed from an alternative promoter in intron 3. *Gene* **251**, 109–122.

Ando H, Mizutani A, Kiefer H, Tsuzurugi D, Michikawa T & Mikoshiba K (2006). IRBIT suppresses IP_3 receptor activity by competing with IP_3 for the common binding site on the IP_3 receptor. *Mol Cell* **22**, 795–806.

Bevensee MO, Schmitt BM, Choi I, Romero MF & Boron WF (2000). An electrogenic Na^+-HCO_3^- cotransporter (NBC) with a novel COOH-terminus, cloned from rat brain. *Am J Physiol Cell Physiol* **278**, C1200–C1211.

Boron WF, Chen L & Parker MD (2009). Modular structure of sodium-coupled bicarbonate transporters. *J Exp Biol* **212**, 1697–1706.

Chesler M (2003). Regulation and modulation of pH in the brain. *Physiol Rev* **83**, 1183–1221.

Durieux ME, Salafranca MN, Lynch KR & Moorman JR (1992). Lysophosphatidic acid induces a pertussis toxin-sensitive Ca^{2+}-activated Cl^- current in *Xenopus laevis* oocytes. *Am J Physiol Cell Physiol* **263**, C896–C900.

Gamper N & Shapiro MS (2007). Target-specific PIP_2 signalling: how might it work? *J Physiol* **582**, 967–975.

Gillo B, Lass Y, Nadler E & Oron Y (1987). The involvement of inositol 1,4,5-trisphosphate and calcium in the two-component response to acetylcholine in *Xenopus* oocytes. *J Physiol* **392**, 349–361.

Gross E, Fedotoff O, Pushkin A, Abuladze N, Newman D & Kurtz I (2003). Phosphorylation-induced modulation of pNBC1 function: distinct roles for the amino- and carboxy-termini. *J Physiol* **549**, 673–682.

Gross E, Hawkins K, Pushkin A, Sassani P, Dukkipati R, Abuladze N, Hopfer U & Kurtz I (2001). Phosphorylation of Ser^{982} in the sodium bicarbonate cotransporter kNBC1 shifts the HCO_3^-:Na^+ stoichiometry from 3:1 to 2:1 in murine proximal tubule cells. *J Physiol* **537**, 659–665.

Heyer M, Müller-Berger S, Romero MF, Boron WF & Frömter E (1999). Stoichiometry of the rat kidney Na^+-HCO_3^- cotransporter expressed in *Xenopus laevis* oocytes. *Pflügers Arch* **438**, 322–329.

Lee MG, Ohana E, Park HW, Yang D & Muallem S (2012). Molecular mechanism of pancreatic and salivary gland fluid and HCO_3^- secretion. *Physiol Rev* **92**, 39–74.

Liu X, Williams JB, Sumpter BR & Bevensee MO (2007). Inhibition of the Na/bicarbonate cotransporter NBCe1-A by diBAC oxonol dyes relative to niflumic acid and a stilbene. *J Membr Biol* **215**, 195–204.

Liu Y, Xu JY, Wang DK, Wang L & Chen LM (2011). Cloning and identification of two novel NBCe1 splice variants from mouse reproductive tract tissues: A comparative study of NCBT genes. *Genomics* **98**, 112–119.

Lupu-Meiri M, Shapira H & Oron Y (1988). Hemispheric asymmetry of rapid chloride responses to inositol trisphosphate and calcium in *Xenopus* oocytes. *FEBS Lett* **240**, 83–87.

McAlear SD & Bevensee MO (2006). A cysteine-scanning mutagenesis study of transmembrane domain 8 of the electrogenic Na/bicarbonate cotransporter NBCe1. *J Biol Chem* **281**, 32417–32427.

McAlear SD, Liu X, Williams JB, McNicholas-Bevensee CM & Bevensee MO (2006). Electrogenic Na/HCO_3 cotransporter (NBCe1) variants expressed in *Xenopus oocytes*: functional comparison and roles of the amino and carboxy termini. *J Gen Physiol* **127**, 639–658.

Müller-Berger S, Ducoudret O, Diakov A & Frömter E (2001). The renal Na-HCO_3-cotransporter expressed in *Xenopus laevis* oocytes: change in stoichiometry in response to elevation of cytosolic Ca^{2+} concentration. *Pflügers Arch* **442**, 718–728.

Oron Y, Dascal N, Nadler E & Lupu M (1985). Inositol 1,4,5-trisphosphate mimics muscarinic response in *Xenopus* oocytes. *Nature* **313**, 141–143.

Perry C, Blaine J, Le H & Grichtchenko II (2006). PMA- and ANG II-induced PKC regulation of the renal Na^+-HCO_3^- cotransporter (hkNBCe1). *Am J Physiol Renal Physiol* **290**, F417–F427.

Perry C, Le H & Grichtchenko II (2007). ANG II and calmodulin/CaMKII regulate surface expression and functional activity of NBCe1 via separate means. *Am J Physiol Renal Physiol* **293**, F68–F77.

Petersen CC & Berridge MJ (1994). The regulation of capacitative calcium entry by calcium and protein kinase C in *Xenopus* oocytes. *J Biol Chem* **269**, 32246–32253.

Romero MF, Fulton CM & Boron WF (2004). The SLC4 family of HCO_3^- transporters. *Pflügers Arch* **447**, 495–509.

Sciortino CM & Romero MF (1999). Cation and voltage dependence of rat kidney electrogenic Na^+-HCO_3^- cotransporter, rkNBC, expressed in oocytes. *Am J Physiol Renal Physiol* **277**, F611–F623.

Shirakabe K, Priori G, Yamada H, Ando H, Horita S, Fujita T, Fujimoto I, Mizutani A, Seki G & Mikoshiba K (2006). IRBIT, an inositol 1,4,5-trisphosphate receptor-binding protein, specifically binds to and activates pancreas-type Na^+/HCO_3^- cotransporter 1 (pNBC1). *Proc Natl Acad Sci U S A* **103**, 9542–9547.

Thornell IM & Bevensee MO (2011). Role of Ca^{2+} in phosphatidylinositol 4,5-bisphosphate (PIP_2)/IP_3-induced stimulation of the electrogenic Na/bicarbonate cotransporter NBCe1-C heterologously expressed in *Xenopus laevis* oocytes. *FASEB J* **25**, 656.6.

Thornell IM, Wu J & Bevensee MO (2010). The IP_3 receptor-binding protein IRBIT reduces phosphatidylinositol 4,5-bisphosphate (PIP_2) stimulation of Na/bicarbonate cotransporter NBCe1 variants expressed in *Xenopus laevis* oocytes. *FASEB J* **24**, 815.6.

Wu J, Liu X, Thornell IM & Bevensee MO (2009*a*). Phosphatidylinositol 4,5-bisphosphate stimulation of electrogenic Na/bicarbonate cotransporter NBCe1 variants expressed in *Xenopus laevis* oocytes. *FASEB J* **23**, 800.13.

Wu J, McNicholas CM & Bevensee MO (2009*b*). Phosphatidylinositol 4,5-bisphosphate (PIP_2) stimulates the electrogenic Na/HCO_3 cotransporter NBCe1-A expressed in *Xenopus* oocytes. *Proc Natl Acad Sci U S A* **106**, 14150–14155.

Yang D, Shcheynikov N & Muallem S (2011). IRBIT: it is everywhere. *Neurochem Res* **36**, 1166–1174.

Yoshida S & Plant S (1992). Mechanism of release of Ca^{2+} from intracellular stores in response to ionomycin in oocytes of the frog *Xenopus laevis*. *J Physiol* **458**, 307–318.

Zeuthen T, Zeuthen E & Klaerke DA (2002). Mobility of ions, sugar, and water in the cytoplasm of *Xenopus* oocytes expressing Na^+-coupled sugar transporters (SGLT1). *J Physiol* **542**, 71–87.

Zhu Q, Kao L, Azimov R, Newman D, Liu W, Pushkin A, Abuladze N & Kurtz I (2010). Topological location and structural importance of the NBCe1-A residues mutated in proximal renal tubular acidosis. *J Biol Chem* **285**, 13416–13426.

Author contributions

All experiments were performed in the laboratory of M.O.B. in the Department of Cell, Developmental and Integrative Biology at the University of Alabama at Birmingham. The contribution of each author to this study is as follows. I.M.T., M.O.B. and J.W.: conception and design of the experiments. I.M.T., J.W., X.L. and M.O.B.: collection, analysis, and/or interpretation of data. I.M.T. and M.O.B.: drafting the article or revising it critically for important intellectual content. All authors approved the final version of the manuscript.

Acknowledgements

We thank Drs Katsuhiko Mikoshiba and Hideaki Ando (RIKEN Brain Science Institute, Japan) for providing the mutant S68A IRBIT construct and relevant information. We also thank Drs Mark D. Parker and Walter F. Boron (Department of Physiology and Biophysics, Case Western Reserve University) for providing the mutant S71A IRBIT construct. This work was supported by an award from the American Heart Association, and by NIH/NINDS R01 NS046653.